JOURNAL OF MATERIALS SCIENCE 27 (1992) 5389–5396

Electron probe microanalysis of Nicalon fibres

S. M. BLEAY, A. R. CHAPMAN, G. LOVE, V. D. SCOTT
School of Materials Science, University of Bath, Calverton Down, Bath BA2 7AY, UK

Electron probe microanalysis of a sample of Nicalon fibre showed it to consist of 54.9 wt% Si, 32.1 wt% C and 11.6 wt% O. Studies of the fine structure of the X-ray emission bands suggested these elements were combined as 46 vol% silicon carbide, 34 vol% silicon oxycarbide and 20 vol% free carbon, with the oxycarbide in the outermost regions of the fibre being significantly richer in oxygen. The silicon carbide was composed of microcrystallites several micrometres in diameter and the remaining material formed an amorphous network of material surrounding the microcrystallites.

1. Introduction

The principle of using high-strength ceramic fibres to reinforce materials such as ceramics and metals has been recognized for many years, but it is only since good quality fibres have been available on a commercial basis that the prospect of using them in composites has become attractive. Nicalon (Nippon Carbon, Japan), developed by Yajima *et al.* in the mid-70s [1, 2], is one such fibre. It is manufactured by pyrolysis of an organo-metallic filament to give an inorganic fibre, diameter $\sim 13\ \mu m$, based upon silicon carbide. Several types of Nicalon fibre have since been produced and their mechanical properties and microstructure have received much study. In addition to silicon carbide, free carbon [3, 4] and silica have been reported to be present, the amount of carbon being found to vary by slightly altering the production process. The degree of crystallinity and crystallite size was also found to differ between production batches, as did Young's modulus and tensile strength of the fibre [5, 6].

There has been consensus that the silicon carbide content of the fibre totals around 65%, whether it is in the microcrystalline form or amorphous with short-range order. The free carbon is believed to exist as microcrystals, estimates from electron spin resonance data giving a microcrystallite size of ~ 2 nm [6], whilst a value of ~ 5 nm was deduced from Raman spectroscopy [7]. Recent transmission electron microscopy studies [8] showed that the carbon existed as a fine network almost completely surrounding the microcrystals of silicon carbide, but it is not easy to find values quoted for the free carbon content. Estimates of up to 20% have been quoted [7] from Raman spectroscopy results, and more than 30% based upon an examination of X-ray photoelectron spectroscopy (XPS) data.

With regard to the form and distribution of oxygen in the fibre, Yajima *et al.* [9] suggested that it was present primarily as a surface layer of silica. Subsequently, using results from electron-probe microanalysis (EPMA) and secondary ion mass spectrometry (SIMS) [6], it was considered that the oxygen was distributed fairly uniformly throughout the fibre, although the existence of a surface layer of silica was not ruled out. Indeed, an oxygen-rich surface layer was detected on flame de-sized fibres using XPS [10] and an amorphous silica layer, ~ 20 nm thick, was located on the surface of some fibres when examined in the transmission electron microscope (TEM) [8]. Attempts to identify the chemical form of the oxygen in the bulk of the fibre have, however, proved inconclusive, some authors [11] reporting the presence of the α-quartz modification of SiO_2 and others deducing, from Raman spectroscopy [7], that the oxygen-containing material was amorphous. As with the carbon analyses, consistent data on percentage concentrations of oxygen in Nicalon fibres are not easy to find.

More recent studies using XPS [3] have proposed that a non-stoichiometric oxycarbide phase, SiO_xC_y, is present in the fibre and that this accounts for most of the oxygen content. The argument was based upon the presence of silicon XPS peaks at positions intermediate between those associated with the binding energies of SiO_2 and SiC. It was further suggested that $\sim 20\%$ of the Nicalon fibre consisted of silicon oxycarbide, with a few per cent at most being silica.

Thus there appears to be an abundance of facts and interpretations but not an unequivocal description of the microstructure of Nicalon fibre types in quantitative terms. In the present paper, EPMA data are presented together with results obtained using analytical transmission electron microscopy of thin sections. The findings are discussed with relation to fibre constituents and element segregation and compared with previously published information on Nicalon fibres.

2. Experimental procedure

The Nicalon fibres, designated batch NL 227, were prepared and studied in several ways.

2.1. Polished transverse sections for EPMA

A number of as-received fibres were first immersed in dilute nitric acid to remove the polymeric size present

0022–2461

on the surface. The de-sized fibres were then mounted in a copper-based conducting resin compound and a transverse section cut, ground and polished using successively finer grades of diamond abrasive. Finishing was carried out with an aqueous suspension of colloidal silica, after which the surface was wiped dry.

Transverse sections through Nicalon fibres were also prepared from a plate of metal matrix composite. The plate was manufactured by infiltration of an unidirectional fibre preform with commercial purity aluminium at a temperature of $\sim 750\,^{\circ}C$ [12]. Mounting and polishing of the section followed the procedure adopted for desized fibres.

The polished specimens were examined in a Jeol JXA 8600M EPMA fitted with wavelength-dispersive spectrometers (WDS). Carbon measurements were carried out using a stearate (STE) crystal ($2d = 10.04$ nm) and silicon measurements with a pentaerythritrol (PET) crystal ($2d = 0.874$ nm). Oxygen measurements were made with a thallium acid phthalate (TAP) crystal ($2d = 2.58$ nm) and a multi-layer analyser, MLA, ($2d = 6.09$ nm). The X-ray emission spectrum was recorded on an X–Y plotter while the analyser was rotated through the appropriate Bragg angle range. Reference standards which were investigated included fibres of glassy carbon and of graphite, α-silicon carbide, β-silicon carbide, and silica. Their surfaces were thoroughly cleaned and coated, at the same time as the polished sections, with a thin (~ 10 nm thick) evaporated layer of gold.

2.2. Thin sections for transmission electron microscopy

All the thin sections studied here were prepared from composite plates. Firstly, a 3 mm diameter disc was cut with a hollow drill and ground to a thickness of ~ 300 μm. The disc was "dimpled" on both sides using a VCR model 500 to leave a double-concave specimen with the centre reduced to ~ 20 μm. It was next thinned by argon ion bombardment in a Gatan Duomill.

TEM examination was carried out in a Jeol JEM 2000 FX system fitted with a Link high-angle thin-window energy-dispersive spectrometer (EDS) and AN 10000 analyser.

2.3. Surface analysis

This work involved EPMA of the surface regions of the de-sized Nicalon fibre using low probe voltages in order to confine the incident electrons to the outermost surface regions. The Jeol JXA 8600M was the primary instrument used in this investigation, although some work was performed on a Jeol 35C SEM fitted with a Link "windowless" energy dispersive detector. De-sized Nicalon fibres were fixed to an aluminium planchette and positioned in the instruments such that the fibre length pointed towards the spectrometer being used for measurement. Accurate positioning was important in order to maintain the correct X-ray take-off angle throughout the experiment.

With the electron beam incident perpendicularly on the surface, readings were taken of the oxygen X-ray emission as the electron beam accelerating voltage was varied between 1.5 and 10 kV. Data were also obtained on a transverse fibre section and silica standard under the same analysis conditions. As with the studies on polished bulk specimens (Section 2.1), the complete emission spectrum for each element was recorded on an X–Y plotter.

3. Results

3.1. Polished transverse sections

3.1.1. X-ray intensity measurements

X-ray emission spectra were recorded using the Jeol JXA 8600M WDS system with the electron probe positioned centrally on a fibre in a polished transverse section. X-ray peak positions, peak heights, and peak widths (full width at half maximum, fwhm) for the constituent elements carbon, silicon and oxygen are given in Table I; the oxygen intensities refer to data obtained using the MLA device because it gave a stronger diffracted intensity for this X-radiation than the TAP crystal. The corresponding X-ray emission data from the reference standards are also included in Table I; only data for the α form of silicon carbide is

TABLE I X-ray emission measurements

Sample	X-radiation	X-ray peak intensity (arb. units)	Measured K_α peak		fwhm (eV)	Analysing crystal
			Wavelength[a] (nm)	Energy (eV)		
	SiK_α	81 521	0.713	1739	2.25	PET
Nicalon	OK_α	18 845	2.388	519	9.97	MLA
	CK_α	12 899	4.414	280.9	9.15	STE
α-SiC	SiK_α	10 700	0.713	1739	2.25	PET
	CK_α	13 230	4.409	281.2	7.46	STE
SiO_2	SiK_α	–	0.713	1739	2.25	PET
	OK_α	55 782	2.389	518.9	9.95	MLA
Glassy carbon	CK_α	–	4.440	279.2	11.51	STE
Graphite	CK_α	–	4.426	280.1	12.24	STE
Nicalon	OK_α	–	2.353	526.9	3.24	TAP
SiO_2	OK_α	–	2.355	526.4	2.60	TAP

[a] Measured wavelengths may not correspond exactly with literature values.

given, but that from β-SiC was indistinguishable. The measurements show significant differences between peak positions and fwhm values for the respective carbon K_α X-ray spectra.

These differences in the carbon profile are more clearly revealed when the X-ray peaks are scaled to the same maxima, Fig. 1. The first point to note is that the position of the carbon peak from Nicalon is the same as that from silicon carbide, whereas the carbon peaks from the two types of carbon are displaced ~ 0.03 nm to a longer wavelength. The fwhm values also differ, although that relating to Nicalon is only slightly greater than that from silicon carbide. In carrying out quantitative analysis the silicon carbide was, therefore, preferred as the standard for carbon.

Conventionally, the starting point for establishing chemical composition is the determination of the X-ray intensity ratio, k, of specimen to standard for the particular X-ray radiation. In the case of carbon, however, it was found that the X-ray intensity ratio, k, was influenced by whether measurements were made using peak heights or peak areas; in the latter case the value was 1.1 times higher. Following previous practice [13], all carbon measurements were recorded using peak areas. For the silicon measurements (PET crystal), the K_α peak shapes were essentially the same for Nicalon and the standard (silicon carbide) so that the k ratio could be established directly from peak intensities. A similar situation existed for the oxygen analyses when using a silica standard provided that

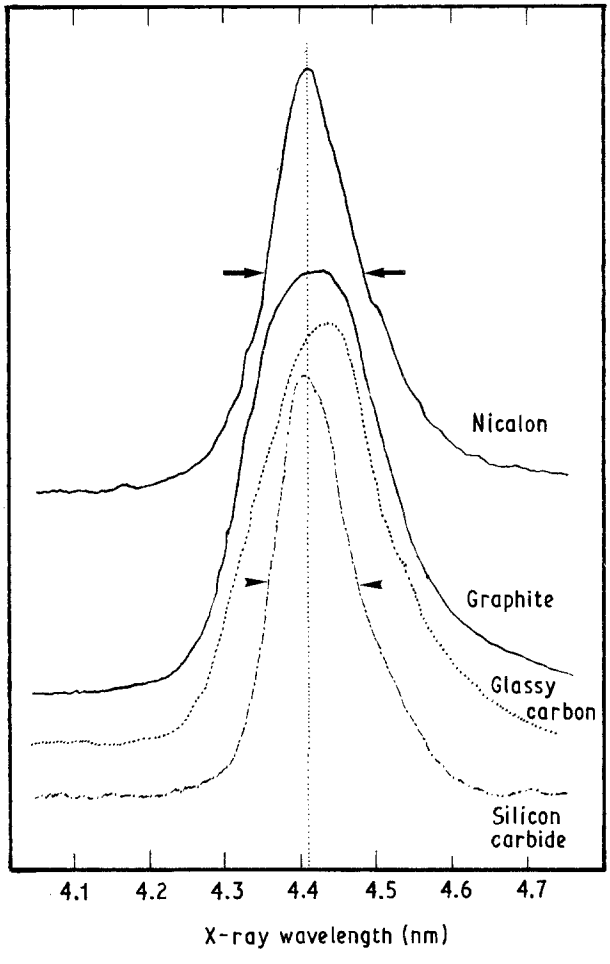

Figure 1 Carbon K_α spectra (normalized); stearate analyser, first order, arrows indicate FWHM.

the MLA crystal, with its relatively poor wavelength resolution, was used as the X-ray analyser. Consequently, here again, peak intensities were used to determine the k ratio.

The experimental measurements were converted into chemical compositions using the Love–Scott ZAF correction model [14] and the X-ray mass absorption coefficients of Heinrich [15]. Weight concentrations for the three elements are collated in Table II for four different fibres within one composite plate, all contained within a single fibre tow. Data for individual fibres are closely similar, elemental concentrations lying within the experimental error of a few tenths of a per cent. It should be pointed out that the totals are all significantly less than 100% and, whilst the possibility of a small systematic error in the ZAF routine cannot be ruled out, it is our contention that some of the small discrepancy may be due to the presence of hydrogen. Certainly no elements apart from those listed could be detected in the Nicalon fibre. The averaged values were 54.87 wt % Si, 11.62 wt % O, and 32.12 wt % C and these were normalized to 55.64 wt %, 11.78 wt % and 32.57 wt %, respectively.

By making an assumption about the form of the oxycarbide, it is possible to gain further insight into the composition of Nicalon fibres. It has been proposed that the oxycarbide is a non-stoichiometric phase consisting of SiO_xC_y tetrahedra (with $x + y = 4$). At the two extremes, therefore, it becomes SiC ($x = 4$, $y = 0$) or SiO_2 ($x = 0$, $y = 4$). To progress we shall take the mid-composition ($x = 2$, $y = 2$) which gives an oxycarbide with the chemical formula $SiOC_{0.5}$. Using the normalized values converted to atomic per cent, Table III, and assuming that all the oxygen (13.55 at %) is associated with an oxycarbide as proposed by Laffon *et al.* [3], then 13.55 at % Si and 6.8 at % C are incorporated in the oxycarbide. Hence, the remaining silicon (23.0 at %) must be linked with carbon to form silicon carbide, leaving 20.1 at % of free carbon. Converting to volume percentages gives 46% SiC, 34% $SiOC_{0.5}$ and 20% free carbon.

3.1.2. X-ray peak shapes

Analysis of Nicalon fibres can be taken one stage further by studying the X-ray emission bands because, as shown above for carbon, low-energy spectra are generally associated with electron transitions from the valence band and are therefore sensitive to the state of bonding of the constituent atoms. These chemical effects are manifested as shifts in the position of the peak maximum, changes in intensity distributions and the occurrence of small satellite peaks.

Returning then to the carbon X-ray spectrum, Fig. 1, it has already been noted that the position and fwhm of the peak from Nicalon resembles more closely that from silicon carbide than either form of carbon. Furthermore, the shape of the high-energy side of the carbon peak from Nicalon falls between that from silicon carbide and the two carbons. This feature is more clearly evinced in the second-order

TABLE II Percentage weight concentrations for four different fibres in a composite plate

Element	Fibre 1	Fibre 2	Fibre 3	Fibre 4	S.D.
Silicon	54.88	54.54	54.96	55.13	0.21
Oxygen	11.61	11.71	11.42	11.72	0.12
Carbon	32.09	31.48	32.52	32.38	0.40
Total	98.58	97.73	98.90	99.23	0.56

TABLE III Averaged and normalized concentrations

Element	Average wt %	Normalized wt %	at %
Silicon	54.87	55.64	36.52
Oxygen	11.62	11.78	13.55
Carbon	32.12	32.57	49.93
Total	98.61	100.00	100.00

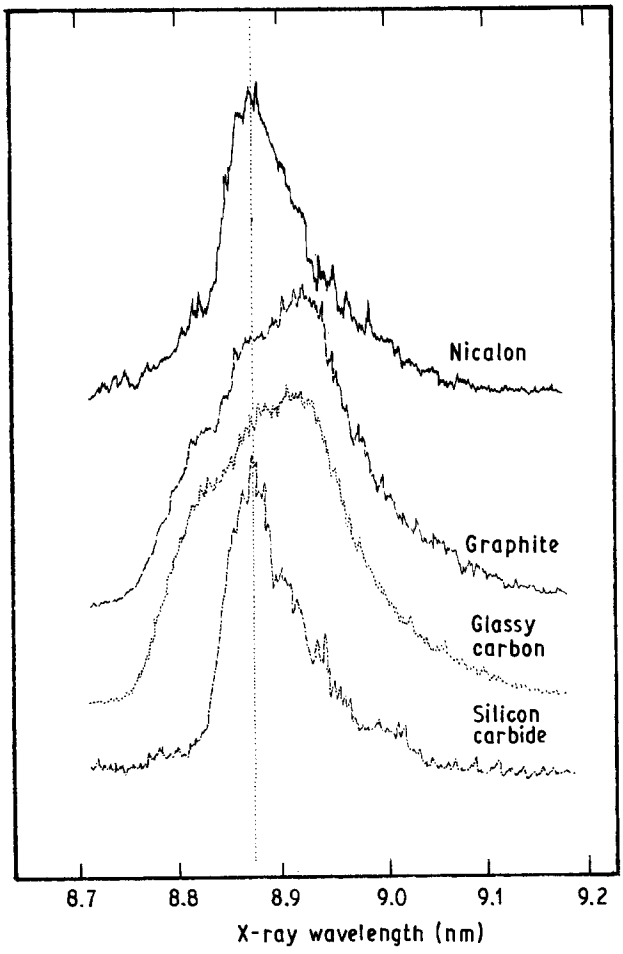

Figure 2 Carbon K_α spectra (normalized); stearate analyser, second order.

carbon spectra, Fig. 2, where spectral dispersion and resolution are improved. The findings clearly indicate that the carbon present in Nicalon is not only chemically bonded to silicon as silicon carbide but also occurs in another form. This is further evidence for the presence of free carbon or oxycarbide in the fibre.

The high-resolution spectra for oxygen, as recorded on the TAP analysing crystal, Fig. 3, are similarly informative. The oxygen spectrum from Nicalon is

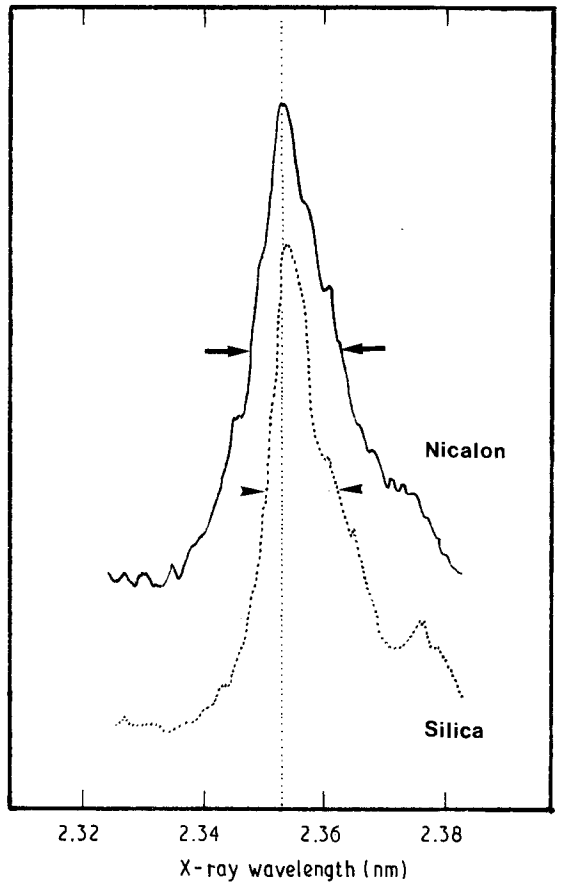

Figure 3 Oxygen K_α spectra (normalized); TAP analyser, arrows indicate fwhm.

significantly different from silica, as evinced by the larger fwhm and the less prominent satellite peak at ~ 2.375 nm. Thus oxygen exists in a form other than silica, which implies the presence of an oxycarbide phase.

With regard to silicon X-rays, the K_α spectrum is not sensitive to the chemical state of the atom and we must turn to the SiK_β emission because this relates to transitions involving the valence electrons. Fig. 4 illustrates the normalized SiK_β spectra from several silicon-containing specimens (silicon, silicon carbide, silicon monoxide, silica and Nicalon). The position of the SiK_β peak from pure silicon (silicon–silicon bonding) is closely similar to that from silicon carbide (silicon–carbon bonding) although the peak is somewhat broader for the latter. Attention is drawn to the small satellite peak at 0.679 nm in the spectrum from silicon carbide, which is evidence of crossover transitions caused by vacancies in the K shell of silicon being filled by electrons from the carbon valence level rather than from the silicon M shell [16]. The SiK_β peak obtained from silica (silicon–oxygen bonding) is

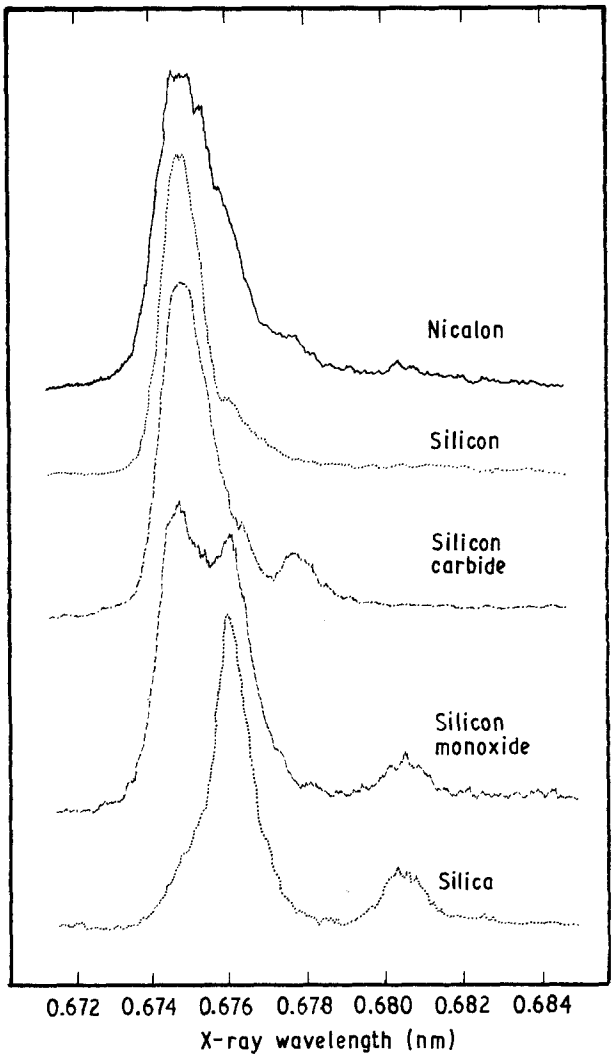

Figure 4 Silicon K_β spectra (normalized); PET analyser.

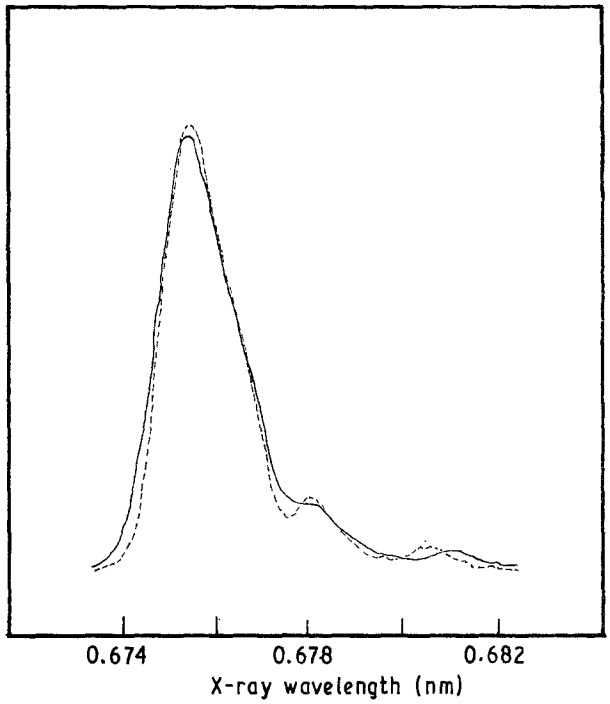

Figure 5 (– – –) Silicon K_β spectra predicted by combining 39.3% of silicon carbide and 31.4% of silicon oxycarbide compared with (——) the spectrum from Nicalon.

at a markedly longer wavelength than that from silicon carbide or silicon, whilst the spectrum from silicon monoxide shows a double peak, one associated with silicon–silicon bonding and the other with the silicon–oxygen bond. In both forms of oxide there is a low-energy satellite peak at 0.682 nm indicative of oxygen–silicon crossover transitions. Thus the broad fwhm value associated with the SiK_β peak for Nicalon, together with its marked asymmetry on its low-energy side, is strong evidence for the presence of both Si–C and Si–O bonding, with the former being predominant.

Using the spectra shown in Fig. 4 it is possible to predict the form of the SiK_β peak from an oxycarbide with the chemical formula $SiOC_{0.5}$. First, a hypothetical peak was deduced by scaling the peaks from SiC and SiO_2 in accordance with their respective weight concentrations of silicon, i.e.

$SiOC_{0.5}$ peak

$$= \frac{1}{2}\left[\frac{0.56}{0.70} \times \text{SiC peak} \times \frac{0.56}{0.467} \times \text{SiO}_2 \text{ peak}\right] \quad (1)$$

Next, proportions of the peaks from $SiOC_{0.5}$ and SiC were added so as to match the SiK_β of Nicalon. The best fit was obtained by taking 39.3% SiC and 31.4% $SiOC_{0.5}$. The final result of the matching process, performed by a least squares analysis on the whole peak profile (some 180 data points), is shown in Fig. 5; the combined spectrum is described by the broken line and the Nicalon spectrum by the full line. The total combined spectra is only 70.7% because of the presence of a non-silicon-bonded element in Nicalon, i.e. free carbon. Translation of the above figures into weight percentages gives 56.7 wt % Si, 14.4 wt % O and 28.9 wt % C, which is in reasonable agreement with the values obtained directly by conventional ZAF corrected EPMA.

3.2. Thin-section studies in the TEM

A transmission electron micrograph taken from the fibre centre, Fig. 6a, shows crystallites of a few nanometres in size. The corresponding selected-area electron diffraction pattern (SAD), Fig. 6b, contains broad rings consistent with the presence of microcrystalline β silicon carbide, a face-centred-cubic structure with $a_0 = 0.436$ nm. The very diffuse central spot is indicative of a substantial amount of amorphous material also being present. EDS data from the same region of the sample, Fig. 6c, show peaks due to carbon, oxygen and silicon. The respective peak intensities accord well with elemental concentrations deduced from the analysis of bulk material, Section 3.1.1, although it was not possible to achieve the same accuracy in the thin section study.

The outer region (~ 200 nm) of fibre curve gave much the same SAD pattern as the fibre interior. The EDS data (Fig. 6d) showed, however, a significantly higher level of oxygen when compared with the fibre interior, whilst the carbon level was correspondingly lower.

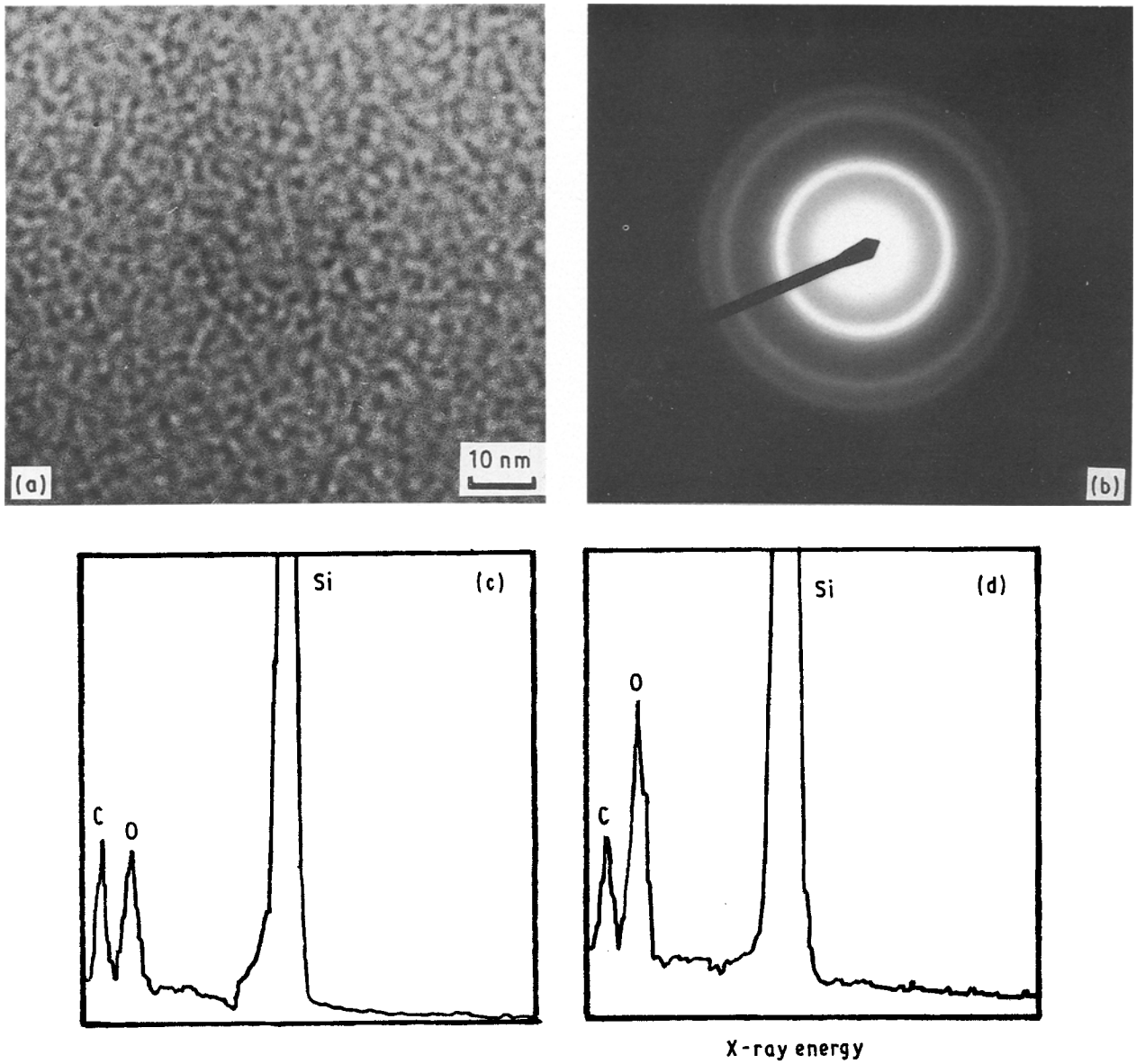

Figure 6 (a) Nicalon fibre; TEM. (b) As (a), SAD. (c) EDS spectrum from fibre core. (d) EDS spectrum from fibre exterior region.

3.3. Surface analysis

To obtain information about the surface composition of the fibre, a low-energy electron beam (2 keV) was directed normally upon the fibre surface and, for reference purposes, at the centre of a transverse section of Nicalon fibre. The respective energy-dispersive X-ray spectra in Fig. 7a and b, show a much higher oxygen/carbon ratio for the fibre surface than its centre. There was some variability in the measurements from different regions of the fibre surface which suggested that the amount of surface oxygen differed significantly over relatively small distances. Additional evidence of oxygen enrichment is given by the Nicalon SiK_β spectrum from the fibre surface (Fig. 8) where the displacement of the peak position to longer wavelengths accords with a greater amount of Si–O bonding compared with Si–C bonding, as expected from the higher level of oxygen.

A measure of the oxygen enhancement at the surface of the fibres is given by the kilovoltage plots of oxygen X-ray intensity from the fibre surface and from the fibre centre, Fig. 9. These show consistently higher X-ray intensities from surface regions of the fibre compared with the centre for all voltages. At very low kilovoltages the ratio is about 2:1, suggesting at least a doubling of the oxygen content compared with the bulk.

This may be due to (a) a higher volume fraction of oxycarbide in the surface regions of the fibre, (b) the presence of a surface film of silica or (c) a higher oxygen:carbon ratio in the outer oxycarbide.

Fig. 10 shows the oxygen intensity ratio from fibre surface to silica standard plotted against kV. The ratio increases as the kV is reduced and the lowest kilovoltage (1.5 kV) is ~ 0.75, which equates with an oxygen concentration of ~ 0.4 wt.% since absorption and atomic number effects can be ignored at low kilovoltages. This value is significantly greater than that of 0.32 predicted for a layer consisting entirely of $SiOC_{0.5}$, which rules out the first possibility. Furthermore, if the surface was silica, the kV plot of oxygen intensity should tend to unity at low voltages. How-

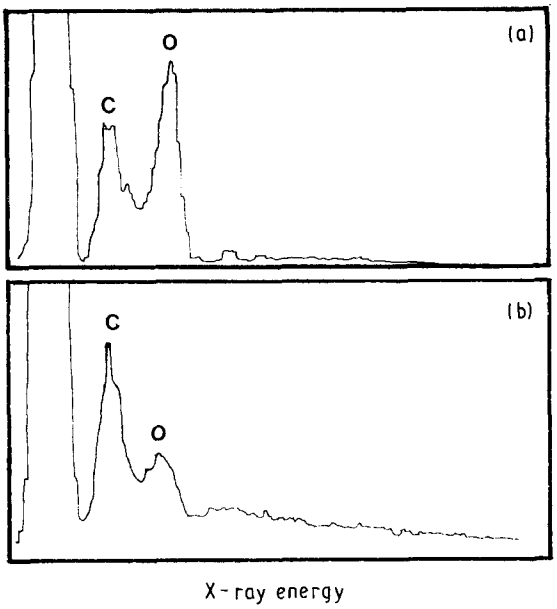

Figure 7 X-ray spectra from (a) fibre surface and (b) core; 2 kV, EDS.

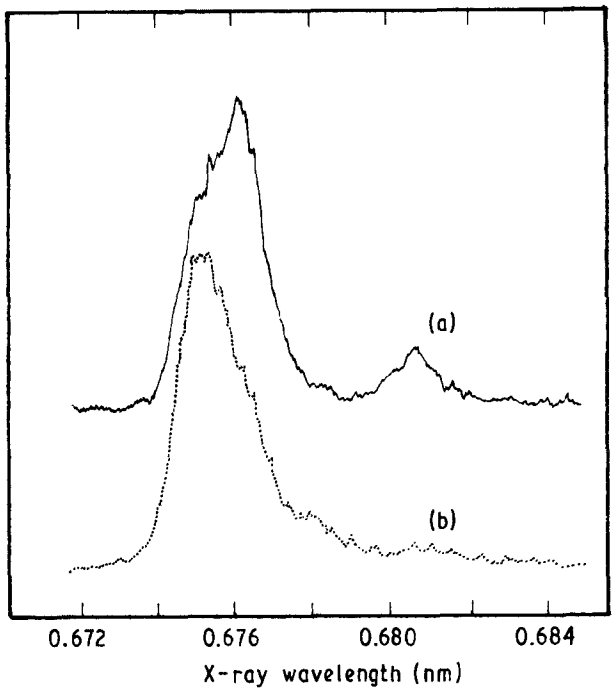

Figure 8 Silicon K_β spectra (normalized) from (a) fibre surface and (b) core; 10 kV, WDS.

ever, calculations using an X-ray excitation depth equation [17]

$$t = 0.033\,(E_0^{1.7} - E_c^{1.7})\,A/\rho Z \qquad (2)$$

(t is in μm, E_0 is accelerating voltage in kV, E_c is critical excitation voltage for oxygen X-rays, A, Z and ρ are mean atomic weight, atomic number and density, respectively, of the surface material) would indicate that the silica layer would have to be less than 50 nm thick to accord with the data. This clearly conflicts with TEM observations of a structure change in the outermost ~200 nm layer. It is, therefore, our contention that the stoichiometry of the oxycarbide changes such that the oxygen: carbon ratio increases towards the fibre surface.

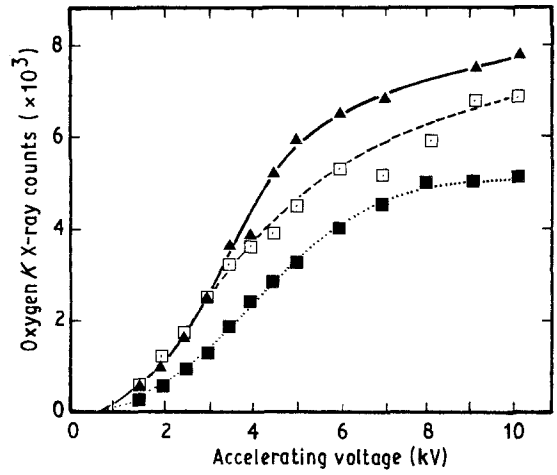

Figure 9 Oxygen K_α intensities from different parts of Nicalon fibre plotted against accelerating voltage, WDS. (▲) Surface 1, (⊡) Surface 2, (■) Core.

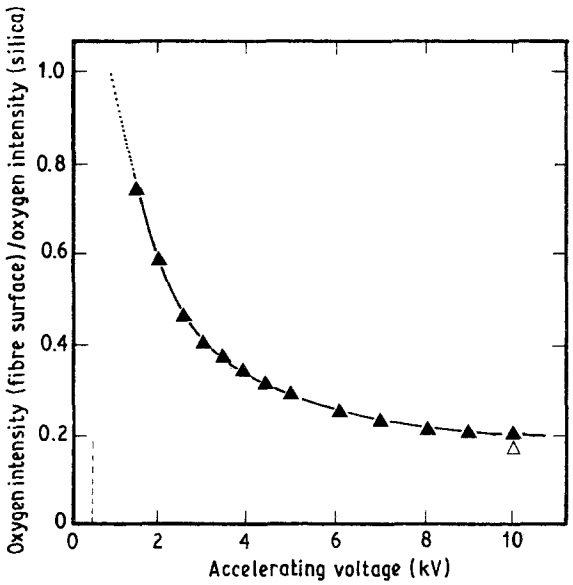

Figure 10 Oxygen K_α intensity ratio of fibre surface to silica, plotted against accelerating voltage, WDS; (△) Value from fibre core. (···) Marks critical excitation energy for oxygen K_α (0.53 keV).

4. Discussion

It has been shown that the Nicalon fibre contains substantial β-SiC in the form of microcrystallites several nanometres in diameter. Much of the material is, however, amorphous in character and this seemingly permeates the fibre as a very fine network surrounding the microcrystallites of silicon carbide.

Electron-probe microanalysis indicated that the fibre consisted of 54.9 wt % silicon, 32.1 wt % carbon and 11.6 wt % oxygen. The data were calculated employing the ZAF correction method proposed by Scott and Love [14], and using peak area measurements where necessary, i.e. the total X-ray spectrum including any satellite lines. The elements present totalled close to 100 wt %, which lends support to the efficacy of the correction procedure adopted in these microanalysis studies. The use of standards (silicon carbide and silica) similar in character to constituents of the Nicalon fibre no doubt helped to produce a self-consistent analysis.

Further useful data were derived from a study of the fine structure of the X-ray emission bands. Comparison of the respective carbon K_α and silicon K_β X-ray profiles from Nicalon and silicon carbide confirmed the presence of substantial silicon carbide as evinced in the electron diffraction pattern, but close inspection of the carbon spectra suggested that free carbon was also present. A similar comparison of the oxygen K_α and silicon K_β peaks from Nicalon with those from silica led to the conclusion that the oxygen was not in the form of silica but was combined in some other way with the silicon and carbon. Thus the presence of a silicon oxycarbide phase was indicated, in accord with findings using X-ray photoelectron spectroscopy [3] and nuclear magnetic resonance [4]. Because oxygen is distributed fairly uniformly throughout the fibre, apart from the superficial (outermost 200 nm) layer of oxygen enrichment, it is considered that the oxycarbide constitutes much of the amorphous phase revealed in the electron diffraction pattern and that it most likely provides the network which surrounds the SiC microcrystallites.

Further analysis of the EPMA results, including X-ray peak matching experiments, led to the conclusion that the Nicalon fibre contained 46 vol % silicon carbide, 20 vol % free carbon and 34 vol % silicon oxycarbide, with an oxycarbide in the outermost ($\sim$ 200 nm) regions which is significantly richer in oxygen.

In later papers, we shall be using these new data to account for the chemical reactions that take place when Nicalon fibre is used to reinforce different types of metal- and ceramic-based composites.

Acknowledgements

The authors thank Rolls Royce plc, the MOD and the SERC for their support.

References

1. S. YAJIMA, H. KAYANO, K. OKAMURA, M. OMORI, J. HAYASHI and K. AKUTSI, *Amer. Ceram. Soc. Bull.* **55** (1976) 1065.
2. S. YAJIMA, K. OKAMURA, J. HAYASHI and M. OMORI *J. Amer. Ceram. Soc.* **59** (1976) 324.
3. C. LAFFON, A. M. FLANK, P. LAGARDE, M. LARIDJANI, R. HAGEGE, P. OIRY, J. COTTERET, J. DIXMIER, J. L. MIQUEL, H. HOWARD and A. P. LEGRAND, *J. Mater. Sci.* **24** (1989) 1503.
4. L. PORTE and A. SARTRE, *ibid.* **24** (1989) 271.
5. C. H. ANDERSON and R. WARREN, *Composites* **15** (1984) 16.
6. G. SIMON and A. R. BUNSELL, *J. Mater. Sci.* **19** (1984) 3649.
7. Y. SASAKI, Y. NISHINA, M. SATO and K. OKAMURA, *ibid.* **22** (1987) 443.
8. Y. MANIETTE and A. OBERLIN, *ibid.* **24** (1989) 3361.
9. S. YAJIMA, K. OKAMURA, T. MATSUZAWA, Y. HASEGEWA and T. SHISHIDO, *Nature* **279** (1979) 706.
10. T. J. CLARK, E. R. PRACK, M. I. HAIDER and L. C. SAWYER, *Ceram. Engng Sci. Proc.* **8** (1987) 717.
11. Y. HASEGAWA and K. OKAMURA, *J. Mater. Sci.* **18** (1983) 3633.
12. R. L. TRUMPER and V. D. SCOTT, in "ECCM 3", edited by A. R. Bunsell, P. Lamicq and A. Massiah (Elsevier, London, New York, 1989) p. 139.
13. G. LOVE, M. G. C. COX and V. D. SCOTT, *J. Phys. D Appl. Phys.* **7** (1974) 2131.
14. V. D. SCOTT and G. LOVE, in "Electron Probe Quantitation", edited by K. F. J. Heinrich and D. Newbury (Plenum Press, New York, 1991), pp. 19–30.
15. K. F. J. HEINRICH, in "X-ray Optics and Microanalysis", edited by J. D. Brown and R. H. Packwood (University of Western Ontario Press, London, Ontario, 1987) pp. 67–119.
16. D. S. URCH, *J. Phys. C* **3** (1970) 1275.
17. R. CASTAING, in "Advances in Electronics and Electron Physics", Vol. 13, edited by L. Marton (Academic Press, New York, 1960) p. 317.

Received 12 December 1991
and accepted 23 January 1992